

# Application of FIDF to the Detection of Unstable Behaviors in Compression Systems

Yew-Wen Liang<sup>1</sup>, Der-Cherng Liaw<sup>2</sup> and Yung-Chun Wu<sup>3</sup>

Department of Electrical and Control Engineering

National Chiao Tung University,

Hsinchu 30039, Taiwan, Republic of China

<sup>1</sup>ywliang@cc.nctu.edu.tw; <sup>2</sup>dcliaw@cc.nctu.edu.tw; <sup>3</sup>ycwu@cc.nctu.edu.tw

## Abstract

Issues concerning the detection of surge and rotating stall in a compression system are studied in this paper. It is observed that the plenum pressure rise and mass flow rate of a compression system exhibit abrupt change due to the appearance of surge or rotating stall, while those of its linearized model do not. With this observation, a linear-based fault identification filter (FIDF) design technique is proposed to detect these two instabilities. This is achieved by treating the difference between the output of the compression system and that of its linearized model at an unstalled operating point as a fault vector and then investigating the effect of the fault on the designed FIDF. Simulation results for Moore and Greitzer's compression model [14] are given to demonstrate the effectiveness of the proposed scheme. The study may provide a means of detecting the occurrence of unstable phenomena at the onset so that a corrective action can be made.

## 1 Introduction

In recent years, the main obstacles to raising the operating efficiency of a compression system are its instabilities. This has generated considerable interest among engineers and researchers in the dynamics and control schemes of such systems (see e.g., [1]-[3], [7, 10, 11], [13]-[16]). Compressed gas is subject to two main kinds of unstable behaviors, surge and rotating stall. The so-called "surge" is characterized as a one-dimensional mass wave motion while "rotating stall" is a wave-like disturbance propagating along the circumferential direction with a constant rotating speed. These two kinds of instability both tend to raise the temperature in the compressor abruptly and may, in some cases, cause extreme mechanical damage. Therefore, distinguishing the causes of surge and rotating stall ([11, 13]), detecting the inception of instability phenomena (see e.g., [3, 10, 15, 16]) and taking appropriate actions to prevent the instabilities (see e.g., [1, 2, 7, 11]) are all important issues. On the other hand, due to the growing

demand for fault detection, diagnosis and identification of a control system, various techniques have been developed (see e.g., [4]-[6] and the references therein). Among these techniques, the so-called "fault detection/identification filter" (FIDF) is one of the most effective (see e.g., [4, 5]). In [5], Ding and Frank proposed an algorithm for designing the FIDF by the use of factorization method in the frequency domain. Later, Chang and Hsu employed the decoupling controller design concept presented in [12] to design the FIDF. This design method is easier to use since it does not require the computation of coprime factorization as mentioned in [5].

The main goal of this paper is to show how the FIDF may be used to detect the occurrence of surge and rotating stall in a compression system. Strictly speaking, surge and rotating stall in a compression system are not faults in the usual sense (see e.g., [5, 6]). However, when surge or rotating stall happens, it is observed that the plenum pressure rise and mass flow rate of the nonlinear compression system exhibit abrupt change while those of its linearized model do not. The idea behind the paper is to treat the difference between the output of the compression system and that of its linearized model as a fault vector and inspect the influence of the fault vector on the residual of the FIDF. With the aid of a linear model-based FIDF design technique [4], the occurrence of surge and rotating stall is shown to be detectable by inspecting the residual generated from the FIDF. For practical applications, the study may provide engineers a signal for when to take appropriate control actions and prevent instability phenomena. Since the employed FIDF technique is simple and easy design, the proposed scheme in this paper is then easier to implement than the existing ones (see e.g., [3, 10, 16]).

The organization of this paper is as follows: Section 2 recalls the FIDF technique. In Section 3, we apply the FIDF technique to the Moore and Greitzer compression model [14] to detect the occurrence of surge and rotating stall. Simulation results are given to demonstrate the use of the approach. Section 4 gives the conclusions.

## 2 THE FAULT IDENTIFICATION FILTER (FIDF)

It is known that one of the most effective approaches to detect the appearance of faults in a control system is through the application of a FIDF (see e.g., [4, 5]). In this section, we recall the FIDF design results presented in [4], which will be employed later to detect the occurrence of surge and rotating stall in compression systems.

Consider a linear plant given by

$$\begin{aligned} \dot{x}(t) &= Ax(t) + Bu(t) + E_1 f(t) & (1) \\ \text{and } y(t) &= Cx(t) + Du(t) + E_2 f(t), & (2) \end{aligned}$$

where  $x(t) \in \mathbb{R}^n$ ,  $u(t) \in \mathbb{R}^m$ ,  $f(t) \in \mathbb{R}^q$  and  $y(t) \in \mathbb{R}^p$  denote the state vector, the input vector, the fault vector and the output vector, respectively. It follows from Eqs. (1) and (2) that

$$y(s) = G_u(s)u(s) + G_f(s)f(s), \quad (3)$$

where

$$\begin{aligned} G_u(s) &= C(sI - A)^{-1}B + D & (4) \\ \text{and } G_f(s) &= C(sI - A)^{-1}E_1 + E_2. & (5) \end{aligned}$$

The objective of FIDF design is to obtain two proper and stable filters  $H_1(s)$  and  $H_2(s)$  such that the residual vector

$$r(s) = H_1(s)u(s) + H_2(s)y(s) \quad (6)$$

has the following property:

$$r(s) = 0 \text{ if and only if } f(s) = 0. \quad (7)$$

The configuration of a FIDF is shown in Figure 1.

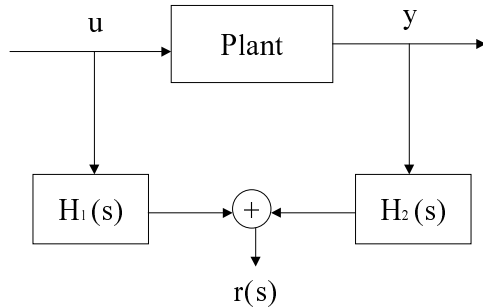


**Figure 1:** FIDF configuration

From Eqs. (3)-(6), we have

$$\begin{aligned} r(s) &= [H_1(s) + H_2(s)G_u(s)]u(s) \\ &\quad + H_2(s)G_f(s)f(s). \end{aligned} \quad (8)$$

To fulfill the requirement of (7), we first assume that  $G_f(s)$  as given by (5) is invertible. The FIDF design procedure given in [4] then can be summarized as the following algorithm.

*Algorithm 1* (FIDF design procedure)

*Step 1:* Construct  $H_2(s)$  so that the transfer matrix

$$H_2(s)G_f(s) \text{ is a diagonal proper and stable one.}$$

*Step 2:* Determine  $H_1(s)$  such that

$$H_1(s) + H_2(s)G_u(s) = 0.$$

*Step 3:* Establish and check  $r(s)$  according to Eq. (6).

Under the procedure of Algorithm 1, it is noted from Eq. (8) that the residual vector is influenced only by the fault vector. Thus, by properly checking the value of residual vector as listed in Step 3 of Algorithm 1 above, one can detect the system fault accurately. In addition to the effect of fault vector, the system output is also affected by nonzero initial state. Since the objective is that the residual be affected only by the fault vector, the response to a nonzero initial state should decay to zero. This implies that the matrix  $A$  in Eq. (1) should also be required to be stable.

## 3 APPLICATION TO COMPRESSION SYSTEMS

In this section, the FIDF technique will be employed to detect the occurrence of surge and rotating stall in a compression system. Strictly speaking, the surge and rotating stall phenomena in compression systems are not faults in the usual sense (see e.g., [5, 6]). However, when surge or rotating stall happens, it is observed that the plenum pressure rise and mass flow rate of the compression system exhibit abrupt change while those of its linearized model do not. Given the significant difference between the states of the nonlinear and linearized models when surge or rotating stall occurs, it is shown that the FIDF technique can be successfully applied to detect the occurrence of surge and rotating stall for compression systems. Details are given below.

Consider a third-order compression system model introduced by Moore and Greitzer [14]:

$$\frac{dA_c}{dt} = \frac{\alpha}{\pi W} \int_0^{2\pi} C_{ss}(\dot{m}_c + W A_c \sin \theta) \sin \theta d\theta, \quad (9)$$

$$\frac{d\dot{m}_c}{dt} = -\Delta P$$

$$+ \frac{1}{2\pi} \int_0^{2\pi} C_{ss}(\dot{m}_c + W A_c \sin \theta) d\theta, \quad (10)$$

$$\frac{d\Delta P}{dt} = \frac{1}{4B_c^2} [\dot{m}_c - F(\gamma, \Delta P)]. \quad (11)$$

The variables and parameters in Eqs. (9)-(11) are de-

scribed as follows:

$\theta$ :	angle along circumference;
$C_{ss}$ :	nondimensional axisymmetric compressor characteristic;
$A_c$ :	amplitude of the first harmonic of asymmetric flow;
$\dot{m}_c$ :	nondimensional compressor mass flow rate;
$\Delta P$ :	nondimensional plenum pressure rise;
$F$ :	inverse function of nondimensional throttle pressure rise;
$\gamma$ :	parameter associated with the throttle opening;
$B_c$ :	nondimensional parameter introduced by Greitzer;
$W$ and $\alpha$ :	two constants.

Suppose the compressor characteristic  $C_{ss}$  is a smooth function of  $\dot{m}_c$ , and solve for the equilibrium points of System (9)-(11). By (9), it is easy to see that  $A = 0$  always results in  $dA/dt = 0$ . However, there may be equilibrium points of (9)-(11) for which  $A \neq 0$  [11]. Denote the equilibrium points for which  $A = 0$  to be  $(0, \dot{m}_c^0(\gamma), \Delta P^0(\gamma))^T$ . The values  $\dot{m}_c^0(\gamma)$  and  $\Delta P^0(\gamma)$  should then satisfy the relationships:  $\dot{m}_c^0 = F(\gamma, \Delta P^0)$  and  $\Delta P^0 = C_{ss}(\dot{m}_c^0)$ . Under the assumption  $A = 0$ , one such equilibrium point  $(0, \dot{m}_c^0(\gamma), \Delta P^0(\gamma))^T$  is referred to as the *unstalled* or *nominal* equilibrium point for the axial flow compression model (9)-(11). Note that this is the normal operating point of the system, the location of which depends on the throttle control parameter  $\gamma$ .

For the demonstration of the application of FIDF technique, in the following we assume that the compressor characteristic  $C_{ss}$  and the inverse of the throttle pressure rise map  $F$  are, respectively, in the following forms [11]:

$$C_{ss}(\dot{m}_c) = 1.56 + 1.5(\dot{m}_c - 1) - 0.5(\dot{m}_c - 1)^3 \quad (12)$$

$$\text{and } F(\gamma, \Delta P) = \gamma\sqrt{\Delta P}. \quad (13)$$

Let  $x_1 = A_c$ ,  $x_2 = \dot{m}_c - 1$  and  $x_3 = \Delta P$ . System (9)-(11) then becomes

$$\dot{x}_1 = 1.5\alpha x_1(1 - x_2^2 - 0.25W^2x_1^2), \quad (14)$$

$$\dot{x}_2 = -x_3 + 1.56 + 1.5x_2(1 - 0.5W^2x_1^2) - 0.5x_2^3, \quad (15)$$

$$\dot{x}_3 = \frac{1}{4B_c^2}(x_2 + 1 - \gamma\sqrt{x_3}). \quad (16)$$

In order to apply the FIDF results [4], we should construct the linearized model of system (9)-(11) about an unstalled operating point  $x_0^T(\gamma_0) = (x_{10}, x_{20}, x_{30})^T$  for some given  $\gamma = \gamma_0$  as follows:

$$\dot{\hat{x}} = A\hat{x} + B\hat{\gamma}, \quad (17)$$

where  $\hat{x} = x - x_0$ ,  $\hat{\gamma} = \gamma - \gamma_0$ ,

$$A_{11} = \frac{3}{2}\alpha(1 - x_{20}^2) - \frac{9}{8}\alpha W^2 x_{10}^2 \quad (18)$$

$$A_{12} = -3\alpha x_{10} x_{20} \quad (19)$$

$$A_{13} = A_{31} = 0 \quad (20)$$

$$A_{21} = -\frac{3}{2}W^2 x_{10} x_{20} \quad (21)$$

$$A_{22} = \frac{3}{2}(1 - x_{20}^2) - \frac{3}{4}W^2(x_{10})^2 \quad (22)$$

$$A_{23} = -1 \quad (23)$$

$$A_{32} = \frac{1}{4B_c^2} \quad (24)$$

$$A_{33} = -\frac{\gamma_0}{8B_c^2\sqrt{x_{30}}} \quad (25)$$

$$\text{and } B = \begin{pmatrix} 0 & 0 & -\frac{\sqrt{x_{30}}}{4B_c^2} \end{pmatrix}^T. \quad (26)$$

Here,  $A_{ij}$  denotes the  $(i, j)$ -entry of  $A$ . Moreover, we assume that the available output of the compression system has the form

$$y = C\hat{x} + D\hat{\gamma}, \quad (27)$$

where  $C \in \mathbb{R}^{p \times n}$  and  $D \in \mathbb{R}^{p \times m}$  are two constant matrices.

It is known that a linear model derived from a nonlinear one is a close approximation only near the operating point. To reduce the influence of the difference between the two models, it is suggested that the unstalled operating point for the compression system be chosen as close to the instability inception point as possible.

Denote  $y_{non}(t)$  and  $y_{lin}(t)$  the output for nonlinear and linear model, respectively. It is noted that the two outputs  $y_{non}(t)$  and  $y_{lin}(t)$  are not equal in general. For the linearized model (17)-(27), it is known that [8]

$$y_{lin}(t) = Ce^{At}\hat{x}(0) + \int_0^t Ce^{A(t-\tau)}B\hat{\gamma}(\tau)d\tau + D\hat{\gamma}(t). \quad (28)$$

Note that the first term on the right hand side of Eq. (28) depends only on the initial state while the second and third terms depend only on the input. Since the operating point is chosen to be an unstalled one, the matrix  $A$  given in (17) is a Hurwitz matrix. It follows that the effect of a nonzero initial state will decay to zero exponentially. That is,  $Ce^{At}\hat{x}(0) \rightarrow 0$  as  $t \rightarrow \infty$ . On the other hand, the input and output of the linearized model has the following relationship (with zero initial state)

$$Y(s) = [C(sI - A)^{-1}B + D]\Gamma(s), \quad (29)$$

where  $\Gamma(s)$  and  $Y(s)$  are the Laplace transforms of  $\hat{\gamma}(t)$  and  $y_{lin}(t) - Ce^{At}\hat{x}(0)$ , respectively. If the throttle opening maintains a constant angle  $\hat{\gamma} = \gamma_1$  (i.e.,

$\gamma = \gamma_1 + \gamma_0$ ), then by the Final Value Theorem (see e.g., [9]) and the stability of  $A$  we have

$$\begin{aligned} & \lim_{t \rightarrow \infty} [y_{lin}(t) - Ce^{At}\hat{x}(0)] \\ &= \lim_{s \rightarrow 0} sY(s) \\ &= \gamma_1 \cdot (-CA^{-1}B + D). \end{aligned} \quad (30)$$

It follows that

$$y_{lin}(t) \rightarrow \gamma_1 \cdot (-CA^{-1}B + D) \text{ as } t \rightarrow \infty. \quad (31)$$

This means that the steady state output of the linearized model is linearly dependent on the input. However, when surge or rotating stall happens, the pressure rise and mass flow rate of the nonlinear model will exhibit abrupt change [11, 13]. With these observations, the idea is to treat the difference  $y_{non} - y_{lin}$  as a fault vector and then apply the FIDF technique to inspect the effect on this fault vector when surge or rotating stall occurs.

To demonstrate the application of the proposed methodology, in the following we present simulation results to verify the effectiveness of the approach. It is known that the state variable  $A$  is hard to measure. In these simulations, we suppose the available states for the compression system are  $\Delta P$  and  $\dot{m}_c$ . The output is then chosen in the form of (27) with

$$C = \begin{pmatrix} 0 & 1 & 0 \\ 0 & 0 & 1 \end{pmatrix} \quad (32)$$

$$\text{and } D = 0 \quad (33)$$

for both the linear and nonlinear models of the compression system. The two filters  $H_1(s)$  and  $H_2(s)$  in the FIDF are then designed for the linearized model (1)-(2) with  $A$  and  $B$  given by (18)-(26),  $E_1 = 0$ ,  $C$  and  $D$  given by (32)-(33) and  $E_2 = I_2$ , where  $I_2$  is the identity matrix of dimension two. Moreover, the values of parameters  $\alpha$ ,  $W$  and  $B_c$  are adopted from [11] as follows:  $\alpha = 0.4114$ ,  $W = 1$  and  $B_c = 0.5$ . It was shown from bifurcation analysis that the surge and rotating stall can occur only when  $\gamma < 1.463$  (see e.g., [7, 11]). This motivates us to select the operating point to be  $\gamma = 1.463$  and  $x_0 = (0, 2.2809, 2.4306)^T$ , which is close enough to the instability inception point and makes the matrix  $A$  given in Eq. (17) to be Hurwitz with eigenvalues  $\{-0.3831; -0.6834 \pm 0.9688i\}$ . Following the FIDF design procedure given in Algorithm 1, in these simulations, the filter  $H_2(s)$  is chosen as

$$H_2(s) = \text{diag} \left\{ \frac{1}{s+1}, \frac{1}{s+1} \right\} \quad (34)$$

while the associated filter  $H_1(s)$  is calculated to be

$$H_1(s) = \begin{pmatrix} \frac{1.68s+0.64}{(s+1)(s^3+1.83s^2+2.02s+0.57)} \\ \frac{1.60s^2+2.11s+0.60}{(s+1)(s^3+1.83s^2+2.02s+0.57)} \end{pmatrix}. \quad (35)$$

Moreover, the initial state is chosen as  $(0.8, 2.5, 2.2)^T$ . Figures 2(a), 3(a) and 4(a) describe the curve of the throttle opening, Figures 2(b), 3(b) and 4(b) show the timing response of the three states, Figures 2(c), 3(c) and 4(c) display the status of the second component of the residual while Figures 2(d), 3(d) and 4(d) exhibit the alarm signal, respectively. The alarm signal can be set to 1 if  $|\text{residual}| > 0.3$  and equal to 0 elsewhere.

It is observed from Figure 2(a) that the throttle opening, in this case, is constant at 1.5 from  $t = 0$  to  $t = 10$ , then the value decreases from 1.5 to 1.1 at  $t = 30$  and maintains that value thereafter. In Figure 2(b), It is seen that the pressure rise  $\Delta P$  and the mass flow rate  $\dot{m}_c$  oscillate after about  $t = 30$  while the amplitude of the first harmonic of asymmetric axis flow  $A_c$  almost retains at zero value. This implies that the system undergoes *surge*. The surge behavior starts after  $t = 30$ . However, the onset of surge becomes visible when  $t \approx 30$ . This is also recognizable from the change in the residual as displayed in Figure 2(c) and 2(d). In Figure 3(a), the throttle is decreasing from the beginning of simulation and maintains constant value 1.1 after  $t = 20$ . It is observed from Figure 3(b) that  $\Delta P$  and  $\dot{m}_c$  approach constant values while  $A_c$  grows after  $t = 20$  and maintains a nonzero constant value after about  $t = 30$ . This means that there is a traveling wave of gas around the annulus of the compressor. It results in a very inefficient operation at constant mean mass flow rate and pressure rise. It is seen from Figure 3(b) that  $A_c$  grows rapidly right after  $t = 20$ . This symptom is reflected in the residual and alarm signal in Figures 3(c) and 3(d). Note that the two simulations agree with the existing theoretic results as given in [7] and [11]. Finally, in Figure 4, we open the throttle while encountering the instability phenomena. It is observed from Figure 4(b) that the rotating stall disappears and the state reaches an equilibrium point after a short time transient. This demonstrates that a proper control action can be applied to diminish the surge or stall behavior when such instabilities can be detected.

From these simulations, it is noted that the surge and rotating stall can be successfully detected by the use of the FIDF technique. By properly adjusting the threshold for generating the alarm signal, the FIDF may provide a precursor of avoiding undesirable effect of these unstable behaviors.

## 4 CONCLUSIONS

In this paper, we have considered the detection of surge and rotating stall with regards to a Moore and Greitzer's compression model. By treating the difference between the output of the compression system and that of its linearized model as a fault vector and employing a linear-based fault identification filter design technique,

it is found that the surge and rotating stall can be successfully detected. For practical applications, the study may provide a warning signal that engineers can use to initiate appropriate control actions to prevent the instability phenomena. Simulations are given to demonstrate the effectiveness of this approach.

### ACKNOWLEDGEMENT

The authors are grateful to the reviewers for their comments and suggestions. This research was supported by the National Science Council, Taiwan, R.O.C. under Grants NSC 88-2212-E-009-020, NSC 88-2212-E-009-022, NSC 89-2212-E-009-041 and NSC 89-2212-E-009-042.

### References

[1] O.O. Badmus, S. Chowdhury, K.M. Eveker, C.N. Nett and C.J. Rivera, "Simplified approach for control of rotating stall Part 1: theoretic development," *Journal of Propulsion and Power*, Vol. 11, No. 6, pp. 1195-1209, 1995.

[2] O.O. Badmus, K.M. Eveker and C.N. Nett, "Control-oriented high-frequency turbomachinery modeling: general one-dimensional model development," *ASME Journal of Turbomachinery*, Vol. 117, pp. 320-335, 1995.

[3] M.M. Bright, H.K. Qammar, H.J. Weigl and J.D. Paduano, "Stall precursor identification in high-speed compressor stages using chaotic time series analysis method," *ASME Journal of Turbomachinery*, Vol. 119, No. 3, pp. 491-499, 1997.

[4] S.-K. Chang and P.-L. Hsu, "Design the fault identification filter via a simplified transfer matrix approach," *Proceeding of the American Control Conference*, pp. 2119-2120, 1992.

[5] X. Ding and P.M. Frank, "Fault detection via factorization approach," *Systems and Control Letters*, Vol. 14, pp. 431-436, 1990.

[6] P.M. Frank and B. Köppen-Seliger, "Fuzzy logic and neural network applications to fault diagnosis," *International Journal of Approximate Reasoning*, Vol. 16, pp. 67-88, 1997.

[7] J.-T. Huang, *Stability Analysis and Control of Compression Systems*, Ph.D. Dissertation, Dept. of Electrical and Control Engineering, Chiao Tung Univ., Taiwan, 1998.

[8] T. Kailath, *Linear Systems*, Prentice Hall, Englewood Cliffs, NJ, 1980.

[9] B.-C. Kuo, *Automatic Control Systems*, Prentice Hall, Englewood Cliffs, NJ, fifth ed., 1987.

[10] P.B. Lawless, K.H. Kim and S. Fleeter, "Characterization of abrupt rotating stall initiation in an axial-flow compressor," *Journal of Propulsion and Power*, Vol. 10, No. 5, pp. 709-715, 1994.

[11] D.-C. Liaw and E.H. Abed, "Active control of compressor stall inception: a bifurcation-theoretic approach," *Automatica*, Vol. 32, pp. 109-115, 1996.

[12] C.-A. Lin and T.-F. Hsieh, "Decoupling controller design for linear multivariable plants," *IEEE Transactions on Automatic Control*, Vol. 36, No. 4, pp. 485-489, 1991.

[13] F.E. McGaughan, "Application of bifurcation theory to axial flow compressor instability," *ASME J. Turbomachinery*, Vol. 111, pp. 426-433, 1989.

[14] F.K. Moore and E.M. Greitzer, "A theory of post-stall transient in axial compression systems. Part I-development of equations," *ASME J. Engine for Gas Turbines and Power*, Vol. 108, pp. 68-76, 1986.

[15] L.-C. Shen, P.-L. Hsu and D.-C. Liaw, "Detect the compressor stall by using the FIDF with multi-level triggered flip-flop logic," *The First Chinese World Congress on Intelligent Control and Intelligent Automation*, Beijing, pp. 1540-1545, 1993.

[16] G. Vachtsevanos, H. Kang, J. Cheng and I. Kim, "Detection and Identification of axial flow compressor instabilities," *Journal of Guidance, Control, and Dynamics*, Vol. 15, No. 5, pp. 1216-1223, 1992.

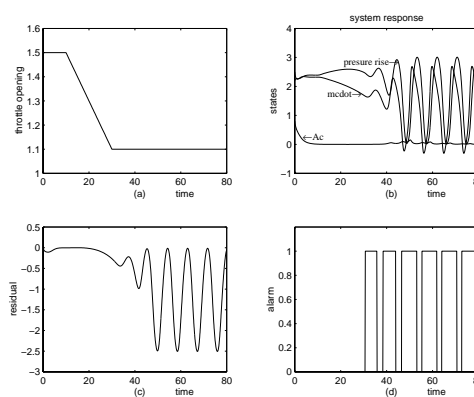


**Figure 2:** (a) Control input; (b) Timing response of system states; (c) residual; (d) Alarm signal

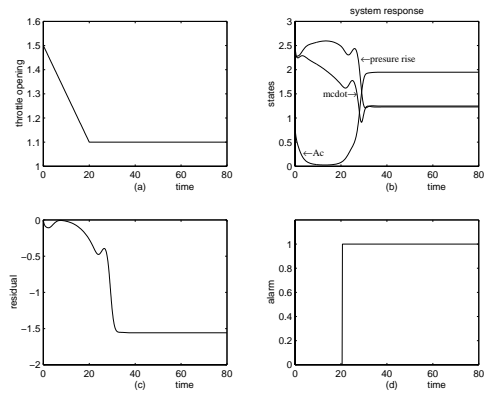


**Figure 3:** (a) Control input; (b) Timing response of system states; (c) residual; (d) Alarm signal

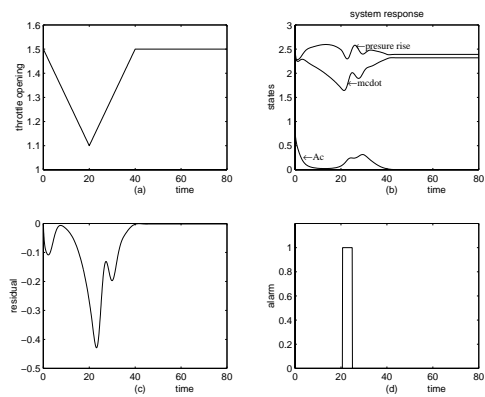


**Figure 4:** (a) Control input; (b) Timing response of system states; (c) residual; (d) Alarm signal